

Human Virus-Derived Small RNAs Can Confer Antiviral Immunity in Mammals

Yang Qiu,^{1,2,3,6} Yanpeng Xu,^{2,6} Yao Zhang,^{4,6} Hui Zhou,^{1,3} Yong-Qiang Deng,² Xiao-Feng Li,² Meng Miao,^{1,3} Qiang Zhang,¹ Bo Zhong,¹ Yuanyang Hu,¹ Fu-Chun Zhang,⁵ Ligang Wu,⁴ Cheng-Feng Qin,^{2,5,*} and Xi Zhou^{1,3,7,*}

¹State Key Laboratory of Virology, College of Life Sciences, Wuhan University, Wuhan, Hubei 430072, China

²State Key Laboratory of Pathogen and Biosecurity, Beijing Institute of Microbiology and Epidemiology, Beijing 100071, China

³Laboratory of RNA Virology, Wuhan Institute of Virology, Chinese Academy of Sciences, Wuhan, Hubei 430071, China

⁴State Key Laboratory of Molecular Biology, Institute of Biochemistry and Cell Biology, Shanghai Institutes for Biological Sciences, Chinese Academy of Sciences, Shanghai 200031, China

⁵Guangzhou Eighth People's Hospital, Guangzhou Medical University, Guangzhou 510060, China

⁶These authors contributed equally

⁷Lead Contact

*Correspondence: qincf@bmi.ac.cn (C.-F.Q.), zhouxi@wh.iov.cn (X.Z.)

<http://dx.doi.org/10.1016/j.immuni.2017.05.006>

SUMMARY

RNA interference (RNAi) functions as a potent antiviral immunity in plants and invertebrates; however, whether RNAi plays antiviral roles in mammals remains unclear. Here, using human enterovirus 71 (HEV71) as a model, we showed HEV71 3A protein as an authentic viral suppressor of RNAi during viral infection. When the 3A-mediated RNAi suppression was impaired, the mutant HEV71 readily triggered the production of abundant HEV71-derived small RNAs with canonical siRNA properties in cells and mice. These virus-derived siRNAs were produced from viral dsRNA replicative intermediates in a Dicer-dependent manner and loaded into AGO, and they were fully active in degrading cognate viral RNAs. Recombinant HEV71 deficient in 3A-mediated RNAi suppression was significantly restricted in human somatic cells and mice, whereas Dicer deficiency rescued HEV71 infection independently of type I interferon response. Thus, RNAi can function as an antiviral immunity, which is induced and suppressed by a human virus, in mammals.

INTRODUCTION

RNAi is an evolutionarily conserved post-transcriptional gene silencing mechanism in eukaryotes (Carthew and Sontheimer, 2009; Kim et al., 2009) and has been well recognized as an innate antiviral immunity in fungi, plants, and invertebrates. In the process of antiviral RNAi, viral dsRNA (double-stranded RNA) replicative intermediates generated during RNA virus replication are recognized and processed by Dicer endoribonuclease into 21- to 23-nucleotide (nt) siRNAs (small interfering RNAs) that contain perfectly base-paired central regions with 2-nt 3' overhangs (Ding, 2010). These virus-derived siRNAs (also named viral siRNAs) are then transferred by Dicer into Argonaute (AGO) proteins, the core components of RNA-induced silencing

complex (RISC), to direct the cleavage of cognate viral RNAs. Thus, the fundamentals of antiviral RNAi immunity are as follows: (1) viral infection induces the production of virus-derived siRNAs, and (2) more importantly, these virus-derived siRNAs or virus-induced RNAi responses have antiviral activity (Cullen et al., 2013; Ding, 2010).

However, when small RNAs in a variety of mammalian somatic cells infected by various RNA viruses, including influenza A virus (IAV) and picornavirus, were subjected to deep sequencing, canonical siRNA species derived from viral RNAs were either not detected or detected at extremely low levels with an overwhelming bias for one strand (Kennedy et al., 2015; Parameswaran et al., 2010; Weng et al., 2014). Additionally, genetic ablation of Dicer or AGO2, the major AGO protein responsible for the siRNA pathway, failed to enhance virus replication in mammalian somatic cells (Bogerd et al., 2014a; Kennedy et al., 2015; Parameswaran et al., 2010). Thus, it remains an open question whether RNAi functions as an antiviral defense in mammals, particularly in differentiated mammalian somatic cells.

Unlike mammalian somatic cells, embryonic stem cells (ESCs) have been found to produce readily detectable siRNAs from long dsRNAs (Nejepinska et al., 2012; Tam et al., 2008; Watanabe et al., 2008). It has been reported that murine ESCs (mESCs) infected by encephalomyocarditis virus (EMCV) produced abundant viral siRNAs, although the differentiation of mESCs resulted in loss of both pluripotency and viral siRNA production (Maillard et al., 2013). Moreover, murine oocytes have been found to express an N-terminally truncated isoform of Dicer that can process dsRNAs into siRNAs (Flemr et al., 2013). Recently, Cullen and colleagues reported that ectopic expression of an N-terminally truncated human Dicer mutant could produce readily detectable viral siRNAs in IAV-infected human somatic cells. However, the shorter Dicer isoform is rodent specific and not naturally present in human cells (Kennedy et al., 2015). Therefore, mESCs and probably certain germline cells, which are undifferentiated and retain some pluripotency, are intrinsically different with differentiated somatic cells in producing siRNAs.

Interestingly, Ding and colleagues found that infection by a Nodamura virus (NoV) mutant that does not express protein B2 triggered the production of readily detectable NoV-derived siRNAs in rodent somatic cell lines and suckling mice (Li et al.,

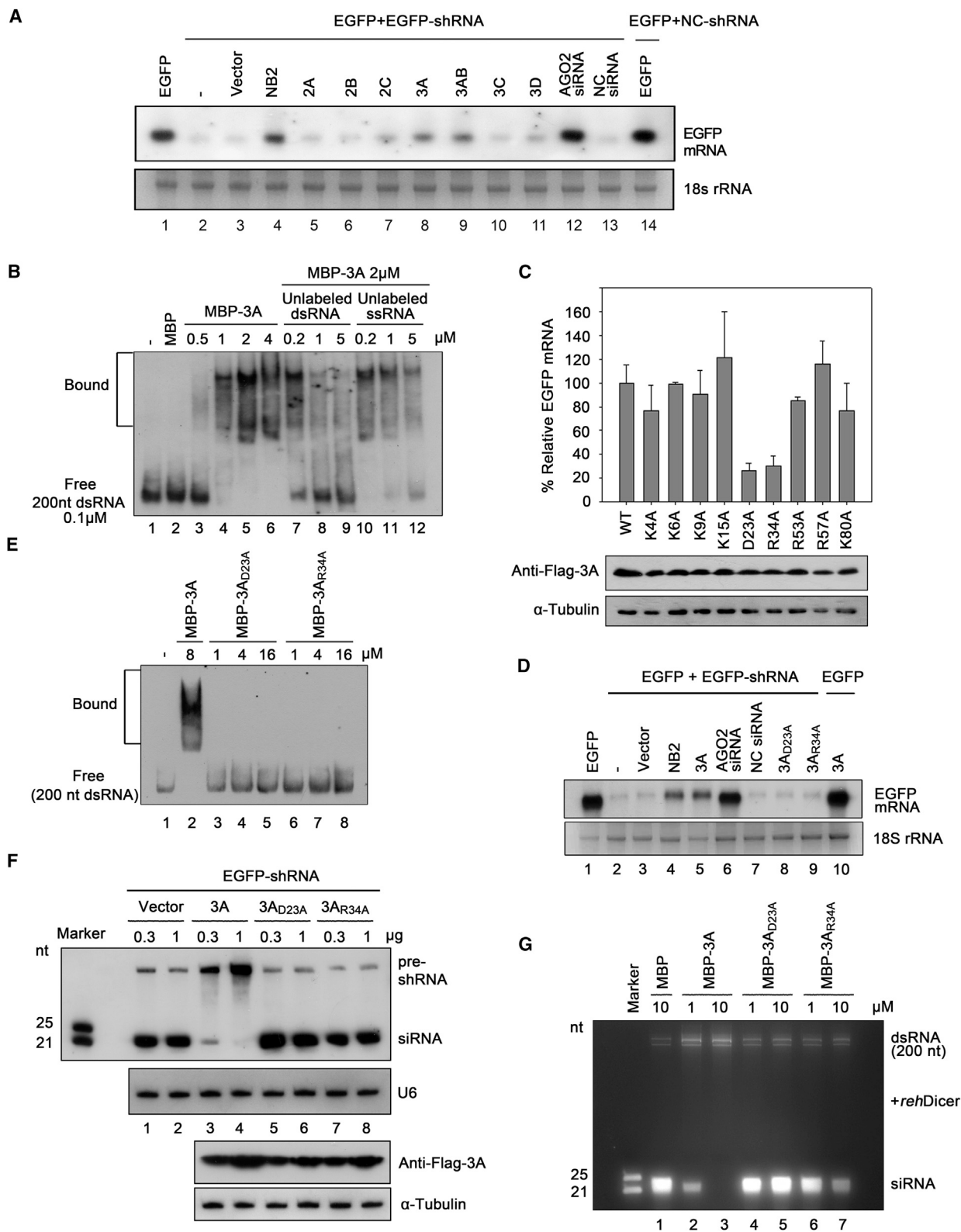


Figure 1. HEV71 3A Suppresses Dicer-Mediated siRNA Biogenesis by Sequestering dsRNA In Vitro

(A) 293T cells were co-transfected with a plasmid encoding EGFP (0.1 μ g) and EGFP-specific shRNA (0.3 μ g), together with either empty plasmid or a plasmid encoding HEV71 nonstructural protein or NoV B2 (NB2) (0.3 μ g for each). Cells transfected with siRNA of AGO2 or NC siRNA (50 nM for each) were used as

(legend continued on next page)

2013). However, NoV is an insect virus, but not a mammalian virus that belongs to the same positive-stranded RNA virus family (*Nodaviridae*) with other insect nodaviruses such as Flock House virus (FHV) and Wuhan nodavirus (Li et al., 2002; Qi et al., 2012). Most insect or plant RNA viruses encode viral suppressors of RNAi (VSRs) to antagonize antiviral RNAi (Ding, 2010). Nodaviral B2 proteins are among the best-characterized VSRs and suppress antiviral RNAi in insects by sequestering viral dsRNAs and targeting RNAi pathway component (Aliyari et al., 2008; Li et al., 2002; Qi et al., 2012). Moreover, some mammalian viral proteins, like IAV NS1 and Ebola virus (EBOV) VP35, have been reported to suppress RNAi in vitro (Haasnoot et al., 2007; Li et al., 2016). Therefore, the identification of an authentic VSR encoded by a mammalian virus would be the key step to answering the fundamental questions: (1) can viral infection induce viral siRNA production?; and (2) does virus-induced RNAi have antiviral activity in mammals?

Enteroviruses are a genus of positive-stranded RNA viruses in the family *Picornaviridae* and include numerous important human pathogens, such as poliovirus, HEV71, echoviruses, and coxsackieviruses that annually infect around 3,000,000,000 people and are responsible for a wide spectrum of diseases. Especially, HEV71 infection in infants and young children causes hand-foot-and-mouth disease (HFMD) and severe neurological manifestations and has emerged as one of the major global threats to public health. In addition, human enteroviruses are among the best-characterized RNA viruses and have served as important models in the development of modern virology (Shih et al., 2011). Here, we first identified the nonstructural protein 3A of HEV71 as the VSR that inhibits Dicer-mediated siRNAs biogenesis by sequestering dsRNAs. When the 3A-mediated suppression of RNAi was impaired by point mutations, the VSR-deficient mutant viruses effectively triggered RNAi response in both mammalian somatic cells and mice, producing abundant HEV71-derived small RNAs with all of the properties of canonical siRNAs. These HEV71-derived siRNAs are Dicer-dependently produced from viral dsRNA replicative intermediates, loaded into AGO-RISC, and are fully active to degrade cognate viral genomic RNAs. Most importantly, the VSR-deficient mutants of HEV71 are significantly restricted in human somatic cells and mice, while Dicer deficiency successfully restored HEV71 infection independently of type I interferon

(IFN-I) response. Overall, our findings highlight that RNAi can indeed function as antiviral immunity in mammals, and here, we showed that it is induced and suppressed by HEV71.

RESULTS

HEV71 Nonstructural Protein 3A Is a Potential VSR

To determine whether HEV71 encodes proteins that work as potential VSRs, we examined all HEV71-encoded nonstructural proteins via a reversal-of-silencing assay. In this assay, cultured human HEK293T cells were co-transfected with the plasmids encoding EGFP and EGFP-specific small hairpin RNA (shRNA), which is cleaved by Dicer to produce siRNA, together with vectors for HEV71 nonstructural proteins. Two days after transfection, EGFP mRNA levels were determined by northern blot (Figure 1A), and the protein expression was determined by western blot (Figure S1A). The EGFP-specific shRNA eliminated the EGFP transcripts (Figure 1A), confirming that the RNAi is effective. We found that the expression of the 3A protein and its precursor 3AB effectively rescued the accumulation of EGFP mRNA, indicating that 3A is a potential VSR (Figure 1A, lanes 8 and 9). In addition, ectopically expressing NoV B2 or knocking down AGO2 (Figure S1B) expectedly inhibited the shRNA-induced RNAi (Figure 1A, lanes 4 and 12; Figure S1C).

Since the RNAi pathway is conserved from plants to animals, we sought to determine if 3A is also able to suppress dsRNA-induced RNAi in insect cells. Our data showed that ectopic expression of HEV71 3A effectively suppressed the dsRNA-induced RNAi in cultured *Drosophila* S2 cells (Figure S1D, lane 5). Moreover, ectopically expressing FHV B2 (FB2), another well-established VSR, or knocking down fly Dicer-2 or AGO2 (Figure S1E) also suppressed RNAi (Figure S1D), as expected.

To further confirm the in vitro RNAi suppression activity of HEV71 3A, we adopted another canonical assay in cultured S2 cells. In this assay, a VSR-deficient mutant of FHV replicon (pFR1-ΔB2) was expressed in S2 cells. Owing to a lack of B2, this mutant replicon was unable to suppress antiviral RNAi, resulting in the near clearance of self-replicated FHV RNA1 and RNA3 in S2 cells (Figure S1F, compared lanes 1 and 2). This replication defect of the VSR-deficient replicon could be partially rescued by the ectopic expression of either FHV B2 or HEV71 3A (Figure S1F, lanes 3 and 4) or by the knockdown of fly AGO2

controls. At 48 hr after transfection, total RNAs were extracted, and the level of EGFP mRNA was examined via northern blotting with DIG-labeled RNA probe targeting the *egfp* ORF 500–720 nt. 18 s rRNA was used as loading control.

(B) Increasing amount (0–4 μM) of MBP-fusion HEV71 3A (MBP-3A) was incubated with 0.1 μM 200-nt DIG-labeled dsRNA at 37°C for 30 min. Complexes were separated on 6% native-PAGE, transferred to membranes, and then incubated with anti-DIG antibody conjugated with alkaline phosphatase. For competition assays, 2 μM of MBP-3A was incubated with 0.1 μM DIG-labeled dsRNA and increasing amounts (0.2–5 μM) of unlabeled dsRNA or ssRNA.

(C) 293T cells were co-transfected with a plasmid encoding EGFP (0.1 μg) and EGFP-specific shRNA (0.3 μg), together with the plasmids encoding HEV71 3A WT or mutants (0.3 μg for each). The EGFP mRNA levels were determined by qRT-PCR with that in the presence of WT 3A defined as 100%. Data represent means and standard deviations (SD) of three independent experiments. Cell lysates were also subjected to western blotting with anti-Flag and anti-α-Tubulin antibodies.

(D) Northern blotting of EGFP mRNA levels of 293T cells co-transfected with a plasmid encoding EGFP and EGFP-specific shRNA, together with either empty plasmid or the plasmid encoding NB2, 3A, or its mutants (3A_{D23A} and 3A_{R34A}).

(E) Increasing amounts (1–16 μM) of MBP-3A_{D23A} or MBP-3A_{R34A} were incubated with 0.1 μM 200-nt DIG-labeled dsRNA at 37°C for 30 min. Complexes were analyzed as noted above.

(F) 293T cells were co-transfected with EGFP-specific shRNA (0.3 μg) and either the increasing amounts (0.1–0.3 μg) of the plasmid encoding 3A or its mutants (3A_{D23A} and 3A_{R34A}). Total RNAs were subjected to northern blotting with either DIG-labeled oligo RNA probe targeting EGFP-shRNA or U6. The synthetic 21- and 25-nt RNAs were used as size markers. Cell lysates were also subjected to western blotting with anti-Flag and anti-α-Tubulin antibodies.

(G) The purified proteins as indicated were incubated with 0.4 μg 200-nt dsRNA together with a human recombinant Dicer (0.5 U) at 37°C for 16 hr. The RNAs were separated on 7 M urea-15% PAGE and visualized by staining with ethidium bromide. Each experiment has been repeated at least three times independently. See also Figure S1.

(Figure S1F, lane 5). Together, these results showed that HEV71 3A can block RNAi in cells and is a potential VSR.

HEV71 3A Suppresses Dicer-Mediated siRNA Biogenesis by Sequestering dsRNA In Vitro

The 3A proteins encoded by poliovirus and Coxsackievirus B3 (CVB3) form a homodimer with each monomer consisting of two antiparallel α helices (Strauss et al., 2003; Wessels et al., 2006) (Figure S1G), which is structurally similar to some VSRs such as nodaviral B2 that sequester dsRNA from Dicer cleavage (Qi et al., 2012). To determine if HEV71 3A binds to long dsRNA, gel shift assays were conducted by incubating in-vitro-transcribed 200-nt digoxin (DIG)-labeled dsRNA with increasing concentrations of recombinant MBP-fusion 3A (MBP-3A, Figure S1H). In addition, unlabeled dsRNAs and ssRNAs were used as competitors to further evaluate the affinities of 3A with dsRNA and ssRNA. The presence of 3A apparently resulted in the gel mobility shift of DIG-labeled dsRNA (Figure 1B, lanes 3–6), and only the unlabeled dsRNAs efficiently competed with DIG-labeled dsRNAs (Figure 1B, lanes 7–9), while the ssRNA competitor had a minimal effect (Figure 1B, lanes 10–12). These results demonstrate that HEV71 3A can bind long dsRNA in vitro.

To identify the critical residues responsible for dsRNA-binding and RNAi suppression activities of HEV71 3A, we performed multiple sequence alignments of the positively charged residues of enterovirus 3As (Figure S1G) and examined the single-point mutations of conserved arginine and lysine using the reversal-of-silencing assay in 293T cells. In addition, because dimerization is required for VSR activities of many plant and insect viruses (Qi et al., 2012), we also introduced a point mutation of Asp23, located in the α 2 helix of 3A, which is identical in all enteroviruses sequenced to date (Figure S1G) and previously reported to be essential for 3A dimerization of poliovirus and CVB3 (Strauss et al., 2003; Wessels et al., 2006). Our data showed that Asp23 was also required for dimerization of HEV71 3A (Figure S1I). Thus, we performed quantitative RT-PCR (qRT-PCR) to determine the effects of different mutants on EGFP mRNA levels and found that mutation of conserved Asp23 or Arg34 to Alanine (D23A or R34A) substantially reduced the ability of 3A to suppress RNAi (Figure 1C). These results were further confirmed by northern blot (Figure 1D, lanes 8 and 9). Furthermore, we found that either the D23A or R34A mutation abolished dsRNA-binding activity of HEV71 3A (Figure 1E), indicating that 3A requires long dsRNA-binding activity to suppress RNAi.

Next, we sought to determine whether HEV71 3A could sequester dsRNA from Dicer cleavage in human somatic cells. Small RNAs were harvested from 293T cells co-expressing shRNA together with 3A or its mutants and then subjected to northern blotting with a DIG-labeled RNA oligo probe that recognizes both the precursor shRNA (pre-shRNA) and mature siRNA. As shown in Figure 1F, the accumulation of \sim 22-nt Dicer-cleaved siRNA was substantially lower in cells expressing 3A than in cells expressing empty vectors. As expected, 3A_{D23A} and 3A_{R34A} failed to suppress the processing of shRNA into siRNA (Figure 1F, lanes 5–8).

To further confirm the direct role of HEV71 3A in protecting dsRNA from Dicer cleavage, we adopted an in vitro assay in which purified 200-nt dsRNA, recombinant human Dicer, and MBP-fusion 3A or its mutants were added. While dsRNA was

efficiently processed into \sim 22-nt siRNA in the presence of MBP alone, MBP-3A_{D23A}, or MBP-3A_{R34A}, the addition of MBP-3A protected dsRNA from cleavage by Dicer in a dose-dependent manner (Figure 1G). Altogether, we conclude that HEV71 3A suppresses RNAi by sequestering dsRNA from Dicer cleavage in vitro.

HEV71 3A Inhibits Dicer-Dependent Production of Virus-Derived siRNAs in Human Somatic Cells

To investigate the VSR function of 3A in an authentic viral infection context, we introduced the D23A or R34A mutation in the 3A coding region of the infectious clone of the HEV71 strain VR1432 (Figure 2A). The wild-type (WT) and mutant viruses were all viable and successfully recovered in human rhabdomyosarcoma (RD) cells (Figures 2B and 2C). The mutant viruses (HEV71_{D23A} and HEV71_{R34A}) showed weaker growth patterns than did the WT virus (HEV71_{WT}) in RD and 293T cells (Figure 2D), suggesting that the loss of VSR function probably contributes to the restriction of HEV71 replication.

The presence of readily detectable viral siRNAs within infected cells has been recognized as a marker of antiviral RNAi (Ding, 2010). To determine if HEV71 infection triggers the production of viral siRNAs, total RNAs were extracted from 293T cells infected with HEV71_{WT} at a multiplicity of infection (MOI) of 10 at 24 hr post-infection (hpi) and then subjected to deep sequencing. Abundant viral small RNAs (vsRNAs), 18–28 nt in length, were detected in the HEV71_{WT}-infected 293T cells (Figure 3A). These vsRNAs failed to cluster as predicted 22 \pm 1-nt Dicer products (canonical siRNAs) but instead were presented as predominantly nonspecific viral RNA degradation products with random size distribution and an overwhelming bias for positive strands (97.38%) (Table S1), similar to those observed in mammalian somatic cells infected by poliovirus and IAV (Kennedy et al., 2015; Parameswaran et al., 2010). Besides, a previous study by Weng et al. identified several HEV71_{WT}-derived vsRNAs that are cleavage products from the internal ribosome entry site (IRES), that vary in size, and that lack siRNA properties (Weng et al., 2014), consistent with our observation.

Next, we infected 293T cells or a characterized Dicer-deficient 293T cell line (NoDice), whose all three copies of the *DICER1* gene are inactivated by gene editing (Bogerd et al., 2014b), with HEV71_{D23A}. Of note, HEV71_{D23A} was used here because the D23A mutation was more efficient than R34A in eliminating the in vitro RNAi suppression activity of 3A (Figure 1G) and restricting HEV71 replication in cells (Figure 2D). As shown in Figure 3A and Table S1, although vsRNAs detected in HEV71_{D23A}-infected cells were less abundant than those in HEV71_{WT}-infected cells, which were likely due to the greatly reduced mutant virus genomic RNA, the positive-strand bias was substantially reduced (67.89%). Moreover, vsRNA reads in 22 \pm 1-nt size were divided approximately equally into positive (59.95%) and negative strands (40.41%), revealing apparent peaks of vsRNAs of both polarities (Figure 3A). Further bioinformatics analysis showed that the HEV71_{D23A} library was enriched for a population of 22-nt vsRNAs that contained a 20-nt perfectly base-paired duplex region with 2-nt 3' overhangs (Figure 3B, peak “–2”), which were not found in the vsRNAs of HEV71_{WT} (Figure 3B). Together, these results show that a significant level of vsRNAs with the properties of canonical siRNAs were

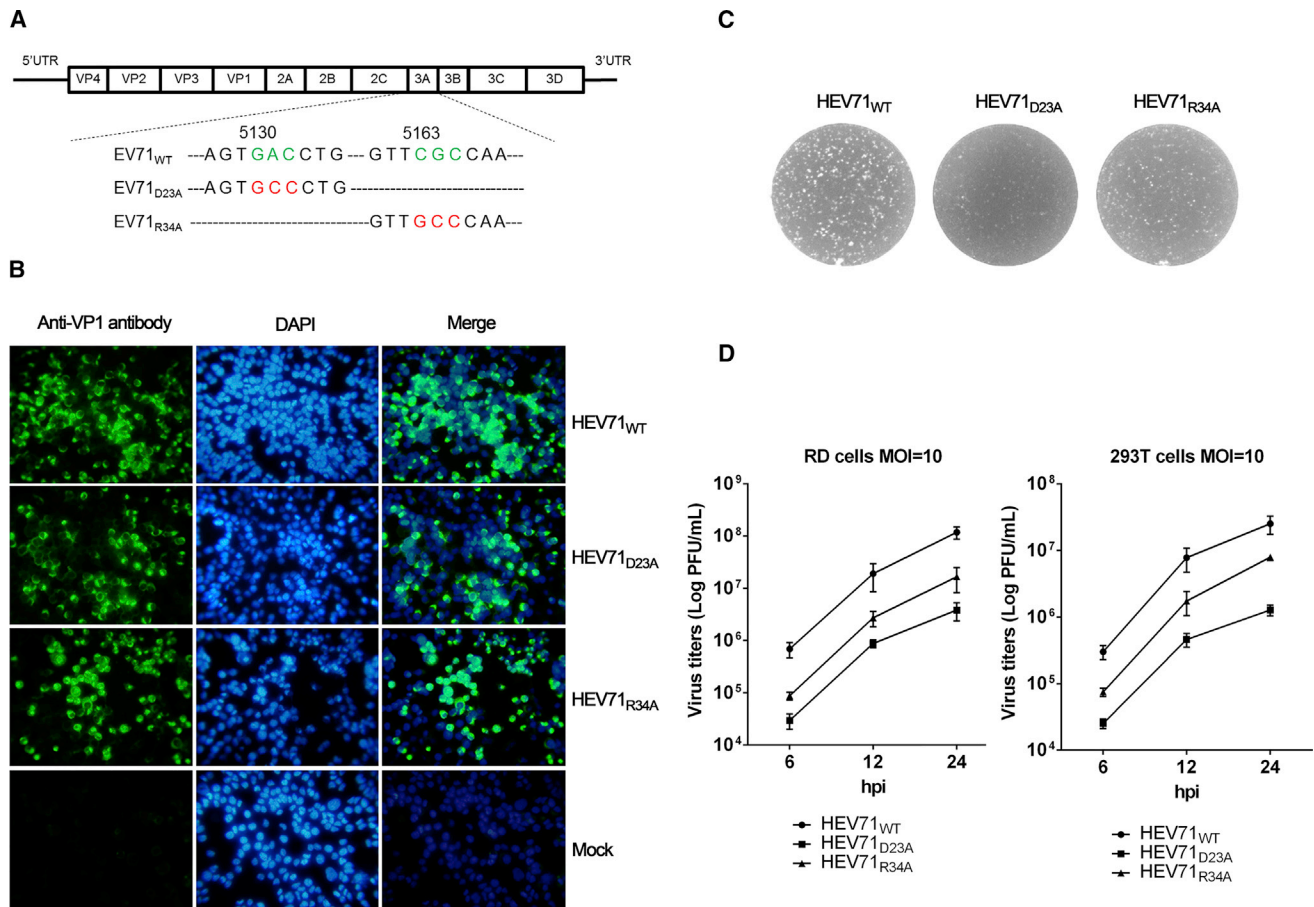


Figure 2. The Replication of 3A-Deficient Mutants of HEV71 Was Inhibited

(A) HEV71 genome and the mutation sites of D23A and R34A of 3A.

(B) RD cells were infected with HEV71_{WT}, HEV71_{D23A}, or HEV71_{R34A} at an MOI of 10. At 24 hpi, cells were subjected to indirect fluorescent assay (IFA) using anti-VP1 antibody (green). The cell nuclei were stained with DAPI (blue). The merged image represents the digital superimposition of green and blue signals.

(C) The plaque morphology of HEV71_{WT}, HEV71_{D23A}, and HEV71_{R34A}.

(D) RD or 293T cells were infected with HEV71_{WT}, HEV71_{D23A}, or HEV71_{R34A} at an MOI of 10. Viral titers were measured at the indicated times using standard plaque assays in RD cells.

produced in 293T cells infected with HEV71_{D23A}, and this finding was also confirmed by an independently repeated experiment (Figures S2A and S2B). Interestingly, when Dicer is deficient by gene editing, far fewer vsRNA reads were detected in NoDice 293T cells infected by HEV71_{D23A} (Table S1), and the remaining vsRNAs did not show any of the siRNA properties observed in normal 293T cells infected with the same mutant virus (Figure 3A and 3B), showing that the production of canonical viral siRNAs is Dicer-dependent.

Analysis of the genomic origin of vsRNA reads predicted to form siRNA duplexes (22-nt size) showed that HEV71_{D23A}-derived siRNAs were highly concentrated at the 5' termini of the HEV71 genome (73.8% of total reads in 22-nt size) in the highly structured IRES (Figure 3C and Figure S2C). Notably, 94.9% of the negative-stranded vsRNA reads in 22-nt size were derived from the terminal regions of antigenomic RNAs (Figure 3C). These terminal vsRNA reads formed successive (or phased) complementary pairs of viral siRNAs (Figures 3D and 3E), and none of the reversed sequences of negative-strand

vsRNA reads from the terminal regions could be mapped to positive-stranded HEV71 genomic RNA (Figure 3F) even when two nucleotide mismatches were allowed, showing that negative-stranded vsRNA reads were derived from antigenomic RNAs produced by viral RNA replication. Together, our results show that the viral siRNAs in HEV71_{D23A}-infected 293T cells were predominantly derived from Dicer processing of the termini of viral dsRNA replicative intermediates, but not viral RNA stem structures.

Production of Abundant Viral siRNAs in Human Somatic Cells Infected with VSR-Deficient HEV71

We next sought to determine whether HEV71-derived siRNAs were abundant enough to be readily detectable by northern blot. Discrete bands in the 21- to 22-nt size range were detected in 293T cells infected with HEV71_{D23A} (Figure 4A, lanes 5–7) by using two different RNA oligo probes complementary to two negative-stranded viral siRNAs (marked by stars in Figure 3E). The HEV71_{D23A}-derived siRNAs also accumulated to high levels

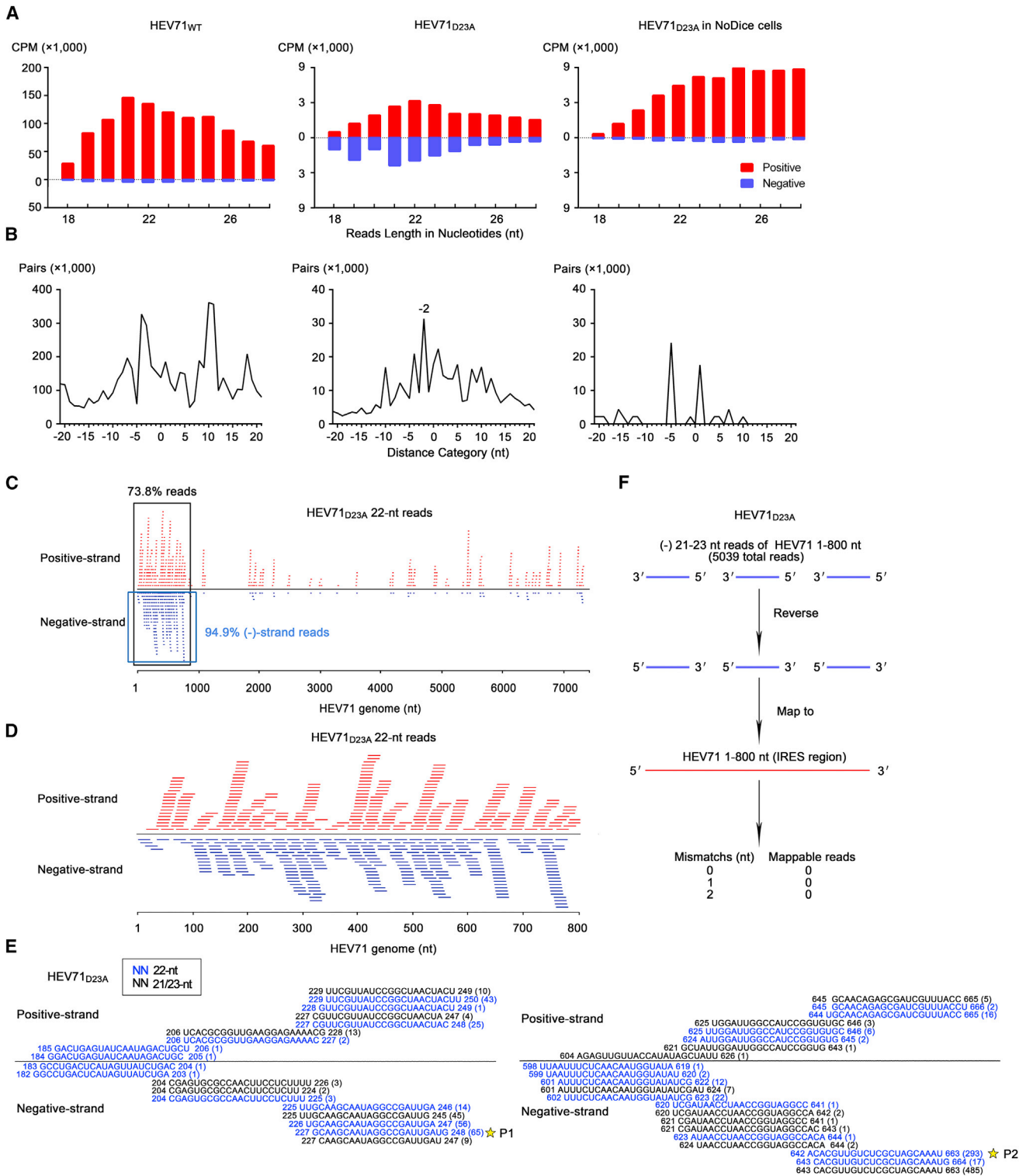


Figure 3. Production of HEV71-Derived siRNAs in Human Somatic Cells

(A) Size distribution and abundance (counts per million of total mature miRNAs, CPM) of total vsRNAs sequenced from 293T cells or NoDice 293T cells infected with HEV71_{WT} or HEV71_{D23A} at an MOI of 10 at 24 hpi. Red, positive-stranded vsRNAs; blue, negative-stranded vsRNAs.

(B) Total pairs of complementary 22-nt vsRNAs derived from HEV71_{WT} or HEV71_{D23A} in each distance category between 5' and 3' ends of a complementary vsRNA pair, showed as -2 for pairs with 2-nt overhang at the 3' end of each strand defined as the canonical viral siRNAs (vsiRNAs).

(legend continued on next page)

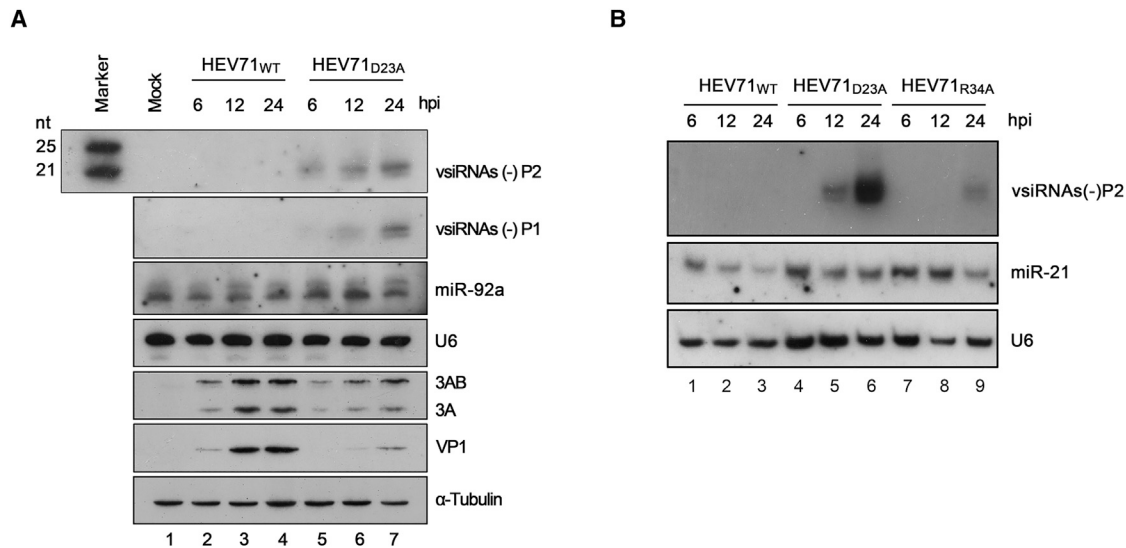


Figure 4. Detection of HEV71-Derived siRNAs by Northern Blot

(A) Northern blot of vsiRNAs in 293T cells infected with HEV71_{WT} or HEV71_{D23A} at an MOI of 10 at 6, 12, and 24 hpi. The two vsiRNA probes were indicated in (A). The same set of RNA and protein samples were used for northern or western blotting to detect miR-92a, U6, viral VP1, 3A and 3AB proteins or α -Tubulin. The synthetic 21- and 25-nt RNAs were used as size markers.

(B) Northern blot of vsiRNAs in RD cells infected with the same titer (MOI = 10) of HEV71_{WT}, HEV71_{D23A}, or HEV71_{R34A} at 6, 12, and 24 hpi.

in human RD cells (Figure 4B, lanes 5 and 6). Moreover, viral siRNAs were also produced in RD cells infected with HEV71_{R34A} (Figure 4B, lane 9). These results provide an independent verification of the production, size, and abundance of the deep-sequenced HEV71-derived siRNAs. In contrast to infection with 3A-deficient HEV71, viral siRNAs were undetectable in either 293T or RD cells infected with HEV71_{WT} (Figure 4A, lanes 2–4; Figure 4B, lanes 1–3), indicating that the biogenesis of the HEV71-derived siRNAs was suppressed by 3A expressed in *cis* from the viral genome, consistent with the results of deep sequencing (Figure 3A).

Together, our findings show that HEV71 3A does function as an authentic VSR in a viral infection context, and when the 3A-mediated suppression of RNAi was genetically impaired in HEV71, RNAi response was effectively induced to produce readily detectable Dicer-dependent viral siRNAs in human somatic cells.

RNAi Plays an Antiviral Role in Human Somatic Cells

Upon confirming that RNAi response could be triggered by infection of VSR-deficient HEV71, but not WT HEV71, we sought to determine if RNAi plays an antiviral role in HEV71-infected human somatic cells. To this end, human 293T or RD cells were infected with WT or VSR-deficient HEV71, and viral RNA accumulation, virus titer, virion production, and viral siRNA pro-

duction were determined. As expected, the viral RNA accumulation and virion production of HEV71_{D23A} or HEV71_{R34A} were restricted in both 293T and RD cells (Figures 5A, 5B, and S3A–S3D), consistent with the virus titer assays (Figures 2D and S4A and S4B). Correspondingly, significant amounts of viral siRNAs, readily detected by northern blot, were produced in cells infected with HEV71_{D23A} or HEV71_{R34A}, but not HEV71_{WT} (Figures 4A, 4B, 5B, and S3B).

Moreover, if RNAi response is indeed antiviral, the rescue of VSR-deficient viruses should be observed in RNAi-compromised cells (Cullen et al., 2013). Our data showed that viral RNA replication and virion production of HEV71_{D23A} or HEV71_{R34A} were rescued by ectopic expression of NoV B2 or HEV71 3A, but not the VSR-deficient mutant of B2 (B2_{R59Q}, also termed “mB2”) or 3A (3A_{D23A}) (Figures 5A, 5B and S3A–S3D). Correspondingly, viral siRNA biogenesis was blocked by ectopic expression of B2 or 3A, but not mB2 or 3A_{D23A} (Figures 5B and S3B, lanes 4–7). More importantly, the deficiency of Dicer in 293T or RD cells efficiently rescued the replication of HEV71_{D23A} or HEV71_{R34A} (Figures 5A, 5B, S3A–S3D, and S4A–S4D). As expected, Dicer deficiency eliminated viral siRNA production (Figures 5B and S3B, lane 8), consistent with our deep sequencing data (Table S1). Therefore, our data show that VSR-deficient viruses can be rescued in

(C) The distribution of vsRNA reads (22-nt size) in the positive- and negative-stranded HEV71 genome and the relative abundances of positive- and negative-stranded vsRNAs are indicated.

(D) A close-up view of the distribution of vsRNA reads in the 5'-terminal 800-nt region of HEV71 genome.

(E) Read sequences along two indicated segments of HEV71 genome. Read counts (in brackets), read length, and genomic position are indicated. The RNAs complementary to the negative-strand vsiRNAs marked by a star were used as the probes for northern blot.

(F) The sequences of negative-stranded HEV71_{D23A}-derived vsRNA reads (5039 reads) in the 5'-terminal regions were reversed and mapped to the sequences of positive-stranded HEV71_{D23A} genome. 0–2 nt mismatches were allowed for mapping.

See also Figure S2 and Table S1.

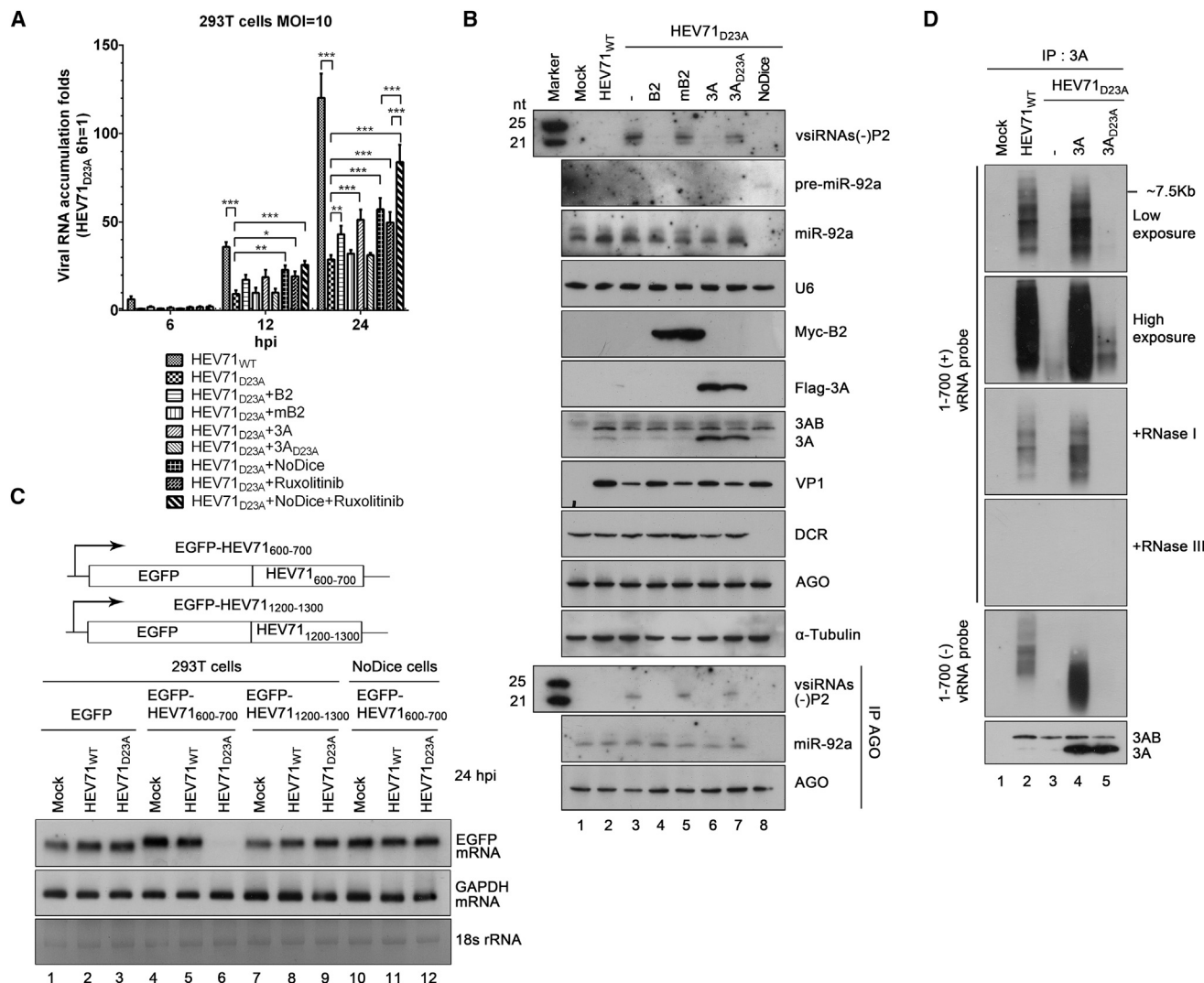


Figure 5. VSR-Deficient HEV71 Triggers Antiviral RNAi Response in Human 293T Cells

(A) 293T or NoDice 293T cells were transfected with expression vector for NoV B2, mB2 (B2_{R59Q}), HEV71 3A, or 3A_{D23A} or treated with Ruxolitinib (2 μ M) as indicated and then infected with HEV71_{WT} or HEV71_{D23A} at an MOI of 10. At 6, 12, and 24 hpi, the levels of HEV71 genomic RNAs were determined by qRT-PCR, and the level of HEV71_{D23A} RNA in 293T cells at 6 hpi was defined as 1. All data represent means and SD of three independent experiments. * $p < 0.05$, ** $p < 0.01$, *** $p < 0.001$ as measured by two-way ANOVA (GraphPad Prism).

(B) 293T cells, NoDice 293T cells, or 293T cells ectopically expressing B2, mB2, 3A, or 3A_{D23A} were infected with the same titer (MOI = 10) of HEV71_{WT} or HEV71_{D23A} at 24 hpi, and the vsRNAs were detected via northern blotting. The same set of RNA and protein samples were used for northern or western blotting to detect precursor miR-92a (pre-miR-92a), miR-92a, U6, ectopically expressed B2 and 3A proteins, HEV71 VP1, 3A and 3AB proteins, host Dicer (DCR) and AGO proteins, or α -Tubulin as indicated. The same cell lysates were subjected to RNA-IP with anti-pan AGO antibody, and western and northern blots were performed to detect precipitated AGO and AGO-bound vsRNAs and miR-92a.

(C) Schematic diagram of the plasmid that transcribes the mRNA containing the *egfp* ORF followed by the 600–700 or 1200–1300 nt region of the HEV71 genome (EGFP-HEV71₆₀₀₋₇₀₀ and EGFP-HEV71₁₂₀₀₋₁₃₀₀). 293T or 293T NoDice cells were transfected with the plasmid encoding either EGFP, EGFP-HEV71₆₀₀₋₇₀₀, or EGFP-HEV71₁₂₀₀₋₁₃₀₀, and 2 hr after transfection, cells were infected with the same titer (MOI = 10) of HEV71_{WT} or HEV71_{D23A}. At 24 hpi, total RNAs were extracted and subjected to northern blotting to detect EGFP mRNA.

(D) 293T cells or 293T cells ectopically expressing 3A or 3A_{D23A} were infected with the same titer (MOI = 10) of HEV71_{WT} or HEV71_{D23A} as indicated. At 24 hpi, cell lysates were prepared and subjected to RNA-IP with anti-3A antibody. The precipitated RNAs were treated in the presence or absence of RNase I or RNase III and then detected by northern blotting using RNA probes targeting positive- and negative-stranded HEV71 genomic 1–700 nt. Precipitated 3A and 3AB proteins were detected by western blots with anti-3A antibody. Each experiment has been repeated at least three times independently.

See also Figure S3, S4, and S5.

RNAi-compromised human somatic cells, and the rescuing effect closely corresponds to the suppression of viral siRNA production.

To evaluate whether 3A plays any role in IFN response, WT or NoDice 293T cells were infected by HEV71_{WT} or HEV71_{D23A}. We found that the induction of IFN- β had no obvious difference at 6

or 12 hpi with either WT or mutant virus and was only moderately more enhanced by HEV71_{D23A} at 24 hpi (Figures S4E and S4F). Additionally, ectopically expressing 3A moderately inhibited polyI:C-stimulated IFN- β induction in 293 cells stably expressing TLR3, comparing with the strong effect of EBOV VP35, a well-known IFN-I antagonist (Figure S4G). Besides, ectopic expression of 3A did not inhibit the induction of IFN-stimulated genes (ISGs) (Figure S4H). Thus, HEV71 3A has a minor inhibitory effect on IFN-I induction in cells.

To exclude the potential interference of IFN-I response, we treated WT or NoDice 293T cells infected by HEV71_{D23A} with Ruxolitinib, a well-known JAK1 and JAK3 inhibitor (Mesa et al., 2012), to block IFN-I response. We found that the RNA accumulation of HEV71_{D23A} in Ruxolitinib-treated Dicer-deficient cells was significantly higher than that in Ruxolitinib-treated WT cells (Figure 5A), showing that the rescuing effect of compromising RNAi on viral replication is independent of IFN-I response.

Interestingly, continuous culturing of HEV71_{R34A} resulted in two different spontaneous mutations, i.e., mutations to WT and Valine (V), and HEV71_{R34V} exhibited similar plaque and growth patterns with HEV71_{WT} and did not trigger viral siRNA production in RD cells (Figure S5), showing that 3A_{R34V} also has VSR activity. The rapid reverse mutations of HEV71_{R34A} are probably due to the pressure of natural selection, further confirming the importance of VSR in viral replication.

Together, our data show that RNAi indeed functions as an antiviral immunity in an IFN-independent manner in human somatic cells.

HEV71-Derived siRNAs Load into AGO and Are Active to Degrade Cognate Viral RNA Sequence

In mammalian RNAi pathway, siRNAs mainly load into AGO2, the only mammalian AGO that exhibits cleavage activity, to guide the destruction of cognate RNA (Liu et al., 2004). To further confirm the antiviral role of virus-triggered RNAi response, we first sought to determine if HEV71-derived siRNAs can load into AGO-RISC. After infection of 293T or RD cells by WT or mutant viruses, small RNAs were subjected to RNA-immunoprecipitation (RNA-IP) with anti-pan AGO antibody. Our results showed that viral siRNAs in cells infected by HEV71_{D23A} or HEV71_{R34A} were co-immunoprecipitated with AGO (Figures 5B and S3B, bottom; Figure S3D, top).

Subsequently, we sought to determine if these HEV71-derived siRNAs are really able to specifically guide the degradation of cognate HEV71 genomic RNAs. Because HEV71 genomic RNAs can self-replicate to generate viral dsRNAs in infected cells, it is difficult to distinguish whether the clearance of HEV71 RNAs is mediated by siRNA-guided AGO cleavage of HEV71 genomic RNA or by Dicer cleavage of HEV71 dsRNAs. To address this issue, we designed a plasmid that transcribes an mRNA containing *egfp* ORF followed by the sequences of 600–700 nt of the HEV71 genome, named “EGFP-HEV71_{600–700}.” This region of the HEV71 genome contains no predicted RNA secondary structure (Figure S2C) and is complementary with a serial of viral siRNAs produced in cells infected with HEV71_{D23A} (Figure 4A). Of note, the plasmid EGFP-HEV71_{1200–1300}, which was constructed using the same strategy but is not complementary with HEV71-derived siRNAs (Figure 3C), was used as a negative control. In addition, the EGFP-HEV71_{600–700} and EGFP-

HEV71_{1200–1300} mRNAs are unable to generate dsRNAs, making them potential targets for HEV71-derived siRNA-guided RNAi, but not Dicer-mediated cleavage. As shown in Figure 5C, the mRNA levels of EGFP-HEV71_{600–700} were substantially reduced by infection with HEV71_{D23A} compared to infection with HEV71_{WT}. By contrast, neither HEV71_{D23A} nor HEV71_{WT} showed any effect in cells expressing EGFP or EGFP-HEV71_{1200–1300} (Figure 5C, lanes 1–3 and 7–9). As expected, HEV71_{D23A}-infection cannot reduce EGFP-HEV71_{600–700} mRNA level in NoDice cells (Figure 5C, lanes 10–12).

In conclusion, HEV71-derived siRNAs indeed load into AGO and are active to guide sequence-specific destruction of cognate viral RNA sequence in a Dicer-dependent manner.

HEV71 3A Sequesters Viral dsRNAs in Infected Cells

Upon confirming that RNAi plays an antiviral role in human somatic cells, we sought to determine if the incapability of HEV71_{WT} to trigger RNAi response and viral siRNA production is indeed due to the VSR activity of 3A in an authentic viral infection context. To this end, we performed RNA-IP with anti-3A antibody in the lysates prepared from 293T cells infected with HEV71_{WT} or HEV71_{D23A}. Total RNAs extracted from the inputs and the RNA-IP products were subjected to northern blotting by using RNA probes targeting positive- and negative-stranded HEV71 genomes 1–700 nt. Viral RNAs of both polarities were readily detected in RNA-IP products from 293T cells infected with HEV71_{WT} (Figure 5D), while the complete viral genomic RNAs were detected in inputs (Figure S3E). The molecular weights of these viral RNAs spanned a broad spectrum, possibly consisting of RNA-IP-enriched replicative intermediates or degradation products (Figure 5D, lane 2). Moreover, the 3A-bound viral RNAs were double-stranded, as they were susceptible to dsRNA-specific RNase III but resistant to ssRNA-specific RNase I (Figure 5D). In addition, ectopically expressed 3A efficiently bound to viral RNAs, which were also double-stranded, in cells infected with HEV71_{D23A} (Figure 5D, lane 4), consistent with our findings that ectopic expression of 3A rescued viral replication and suppressed viral siRNA biogenesis of VSR-deficient HEV71. On the other hand, both virally and ectopically expressed 3A_{D23A} barely associated with HEV71 dsRNAs in cells infected with HEV71_{D23A} (Figure 5D, lanes 3 and 5). Together, our data show that HEV71 3A sequestered viral dsRNAs and could explain why virus-derived siRNAs were barely detectable in human somatic cells infected with WT virus whose VSR activity is potent and intact.

Antiviral RNAi Restricts VSR-Deficient HEV71 Replication in Primary Somatic Cells and in Mice

We sought to expand our evaluation of viral siRNA biogenesis and antiviral effects of RNAi in primary somatic cells and animals. To this end, primary murine lung fibroblasts (MLFs) were isolated from 8- to 10-week-old WT or *Irfnar1*^{-/-} C57/B6 mice and infected with WT or D23A HEV71, respectively. Our data showed that the VSR deficiency substantially restricted the viral replication and virion production of HEV71 in WT or *Irfnar1*^{-/-} MLFs at 12 or 24 hpi (Figures 6A and 6B), consistent with our observations in human 293T and RD cells (Figures 5 and S3). In addition, infection with HEV71_{D23A} triggered the production of HEV71-derived siRNAs, which were readily detectable via northern blotting, in

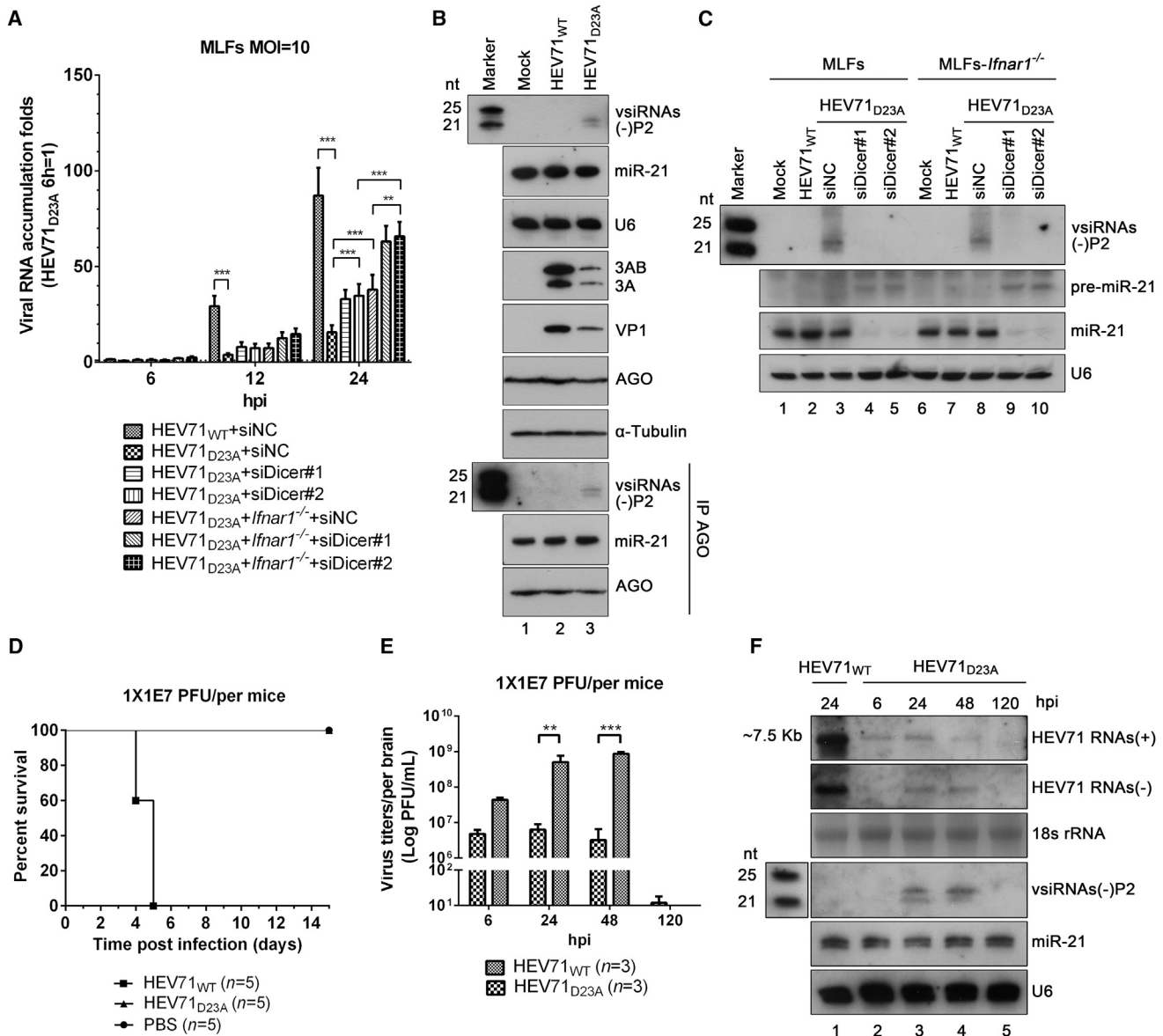


Figure 6. VSR-Deficient HEV71 Triggers Viral siRNA Production and Shows Reduced Viral Replication and Pathogenicity in both MLFs and A129 Mice

(A) Primary WT or *Ifnar1*^{-/-} MLFs, or WT and *Ifnar1*^{-/-} MLFs with Dicer knockdown via siRNAs (siDicer#1 and siDicer#2), were infected with HEV71_{WT} or HEV71_{D23A} at an MOI of 10. At 6, 12, and 24 hpi, the levels of HEV71 genomic RNAs were determined by qRT-PCR with that of HEV71_{D23A} in WT MLFs at 6 hpi defined as 1. All data represent means and SD of three independent experiments. **p* < 0.05, ***p* < 0.01, ****p* < 0.001 as measured by two-way ANOVA (GraphPad Prism).

(B) Northern blotting of vsRNAs in WT MLFs infected with the same titer (MOI = 10) of HEV71_{WT} or HEV71_{D23A} at 24 hpi. The same set of RNA and protein samples were used for northern or western blots to detect miR-21, U6, viral VP1, 3A and 3AB proteins, and α -Tubulin. The same cell lysates were subjected to RNA-IP with anti-pan AGO antibody, and western and northern blots were performed to detect precipitated AGO and AGO-bound vsRNAs and miR-92a.

(C) Northern blotting of vsRNAs in WT or *Ifnar1*^{-/-} MLFs, or WT and *Ifnar1*^{-/-} MLFs with Dicer knockdown infected with the same titer (MOI = 10) of HEV71_{WT} or HEV71_{D23A} at 24 hpi. The same set of RNA samples were used for northern blots to detect precursor miR-21 (pre-miR-21), miR-21, and U6.

(D) Groups of 1-day-old *Ifnar1*^{-/-} A129 mice (*n* = 5) were intracerebrally injected with 1×10^7 PFU of HEV71_{WT} or HEV71_{D23A}. The mortalities were monitored for 15 days or until death. The significance between survival curves from each group was analyzed by Kaplan-Meier survival analysis with log-rank tests.

(E) Groups of 1-day-old *Ifnar1*^{-/-} A129 mice (*n* = 3) intracerebrally injected the same titer of the viruses as noted in (D) were dissected at 6, 24, 48, and 120 hpi. Mouse brains were collected, homogenized, and then subjected to standard plaque assays for determining the viral titers. **p* < 0.05, ***p* < 0.01, ****p* < 0.001 as measured by two-way ANOVA (GraphPad Prism).

(F) Total RNAs were extracted from the same mouse brain samples as noted in (E) and subjected to northern blotting with RNA probes targeting positive- or negative-stranded HEV71 genomic RNAs, viral siRNAs, miR-21, or U6. Ten times more RNAs were loaded for the detection of negative-stranded HEV71 genomic RNAs than for positive-stranded genomic RNAs. 18 s rRNA was used as loading controls. Each experiment has been repeated at least three times independently.

See also Figure S6.

WT or *Ifnar1*^{-/-} MLFs (Figures 6B and 6C), while HEV71_{WT} failed to do so (Figures 6B and 6C). Besides, our RNA-IP assay revealed that viral siRNAs produced in HEV71_{D23A}-infected MLFs also loaded into AGO (Figure 6B, lane 3, bottom).

Moreover, although IFN- β induction was moderately more enhanced by HEV71_{D23A} than by HEV71_{WT} in WT MLFs (Figure S6C), consistent with our observation in 293T cells (Figures S4E and S4F), the knockdown of Dicer in either WT or *Ifnar1*^{-/-} MLFs (Figure S6A) efficiently rescued the replication of HEV71_{D23A} (Figures 6A and S6B), further confirming that the antiviral role of RNAi is independent of IFN-I response. Besides, the Dicer deficiency expectedly eliminated the production of viral siRNAs in either cells (Figure 6C).

Next, we determined the different antiviral responses against the WT and VSR-deficient mutant of HEV71 in *Ifnar1*^{-/-} A129 mice that lack IFN-I receptors. Of note, the usage of *Ifnar1*^{-/-} mice can exclude the potentially different effects of IFN-I response against the WT and mutant virus (Goubau et al., 2013). Groups of 1-day-old A129 mice were intracerebrally challenged with 1×10^7 PFU of HEV71_{WT} or HEV71_{D23A}; and the mortalities of the infected mice were monitored for 2 weeks. As shown in Figure 6D, the HEV71_{WT}-infected mice all died within 5 days, whereas the HEV71_{D23A}-infected mice all survived.

Mouse brains derived from HEV71_{WT}- or HEV71_{D23A}-infected A129 mice at 6, 24, 48, and 120 hpi were extracted, and the virus titers were determined, showing that the replication of HEV71_{D23A} was substantially restricted compared to that of HEV71_{WT} (Figure 6E). Additionally, although the positive-stranded HEV71 genomic RNAs were accumulated at high levels at 24 hpi in the brains of HEV71_{WT}-infected mice (Figure 6F, lane 1), they were accumulated at lower levels from 6–48 hpi and then reduced to an almost undetectable level at 120 hpi during HEV71_{D23A} infection (Figure 6F, lanes 3–5). Besides, negative-stranded antigenomic RNAs became readily detectable at 24 and 48 hpi of HEV71_{D23A} (Figure 6F, lanes 3 and 4), showing that HEV71_{D23A} RNAs replicated but were rapidly cleared in infected mice. Furthermore, we found that the production of viral siRNAs was triggered by infection of A129 mice with HEV71_{D23A}, but not HEV71_{WT}, at 24 and 48 hpi (Figure 6F, lanes 3 and 4). The viral siRNAs became undetectable at 120 hpi (Figure 6F, lane 5), coinciding with the clearance of the replication products (i.e., genomic and antigenomic RNAs) of HEV71_{D23A} (Figure 6F, lane 5).

In summary, our findings show that, similarly to that in human somatic cells, VSR-deficient HEV71 triggered the production of readily detectable virus-derived siRNAs, which was closely associated with viral clearance and dramatically reduced pathogenicity, in a Dicer-dependent but IFN-independent manner both in primary mammalian somatic cells and mice.

DISCUSSION

It has been unclear whether infection by any mammalian viruses would induce and suppress antiviral RNAi response in mammals, mostly because mammalian somatic cells infected by diverse WT mammalian RNA viruses failed to produce readily detectable viral siRNAs or only express very low levels of vsRNAs that lack siRNA properties and are likely random degradation products of viral genomic RNAs. To solve this enigma, several possibilities

have been proposed (Cullen et al., 2013; Kennedy et al., 2015; Li et al., 2013).

One possibility is that WT Dicer expressed in mammalian somatic cells may lack the ability to produce siRNAs from long dsRNAs. This possibility is partly supported by previous findings that the N-terminal helicase domain of mammalian Dicer plays an autoinhibitory role on its siRNA processing activity (Flemr et al., 2013; Ma et al., 2008), and ectopic expression of an N-terminally truncated human Dicer mutant could produce viral siRNAs in human somatic cells infected by IAV (Kennedy et al., 2015). Moreover, it has been suggested that undifferentiated murine cells, like mESCs and oocytes, express an N-terminally truncated isoform of murine Dicer (Nejepinska et al., 2012; Tam et al., 2008; Watanabe et al., 2008), which may explain why mESCs produced viral siRNAs in response to EMCV infection (Maillard et al., 2013). However, these observations do not exclude the possibility that WT Dicer retains some siRNA producing ability. Indeed, although the short Dicer isoform is not naturally expressed in human or murine somatic cells, our data show that viral siRNAs were produced abundantly in human or murine somatic cells and mice infected by VSR-deficient HEV71, demonstrating that WT Dicer is still able to process viral dsRNAs into siRNAs. It is noteworthy that our finding and the aforementioned possibility are not mutually exclusive, as the N-terminal domain may partially inhibit but not abolish siRNA production, and such an autoinhibition of Dicer may be regulated by viral or host factors.

The other possibility is that in the context of viral infection, viruses encode VSRs as an immune evasion mechanism that suppresses viral siRNA production in mammalian somatic cells. This possibility has been discussed (Cullen et al., 2013; Kennedy et al., 2015; Li et al., 2013; Maillard et al., 2013) and supported by recent studies in which readily detectable viral siRNAs were observed in mammalian somatic cells infected with a B2-deficient NoV or NS1-deleted IAV (Li et al., 2016; Li et al., 2013). However, NoV is an insect nodavirus, while IAV NS1 is a well-characterized IFN antagonist, and NS1 deletion did not prevent IAV from replicating and inducing disease and death in IFN-defective mice (Garcia-Sastre et al., 1998). Thus far, the strongest evidence is the identification of HEV71 3A as an authentic VSR. Enteroviral 3A and its precursor 3AB are critical components of viral RNA replication complex (Teterina et al., 2011), while their exact functions in viral RNA replication remain unclear (Gao et al., 2015). We found that infection by VSR-deficient mutant of HEV71 triggered the Dicer-dependent production of viral siRNAs in different human or murine somatic cells, as well as in vivo. Moreover, during HEV71 infection, virally expressed 3A did bind HEV71 dsRNAs in human somatic cells, while VSR-deficient 3A mutant failed to do so. Interestingly, the VSR activity of 3A appears to be under high pressure of natural selection, as a VSR-deficient mutant of HEV71 (HEV71_{R34A}) exhibited rapid spontaneous reverse mutations, further confirming the importance of VSR for HEV71 replication.

The production of abundant virus-derived siRNAs clearly shows that viral dsRNA replicative intermediates are indeed processed by Dicer in mammals. However, these findings only provide compelling evidence, but not direct demonstration, of

antiviral RNAi in mammals, and extra evidence is required to show that virus-induced RNAi does have antiviral activity: first, VSR-deficient viruses should be rescued by genetic ablation of key RNAi component; second, viral siRNAs should load into RISC and be active to degrade cognate viral RNAs. Although previous studies using NoV, EMCV, or IAV did not address this issue (Li et al., 2016; Li et al., 2013; Maillard et al., 2013), our findings show that HEV71-derived siRNAs load into AGO2-RISC and are fully active to degrade cognate HEV71 RNA sequence and VSR-deficient mutant of HEV71 is significantly restricted in human somatic cells, primary somatic cells and mice, while Dicer deficiency successfully rescues mutant HEV71 replication.

In addition to being recognized by Dicer, viral dsRNAs are usually recognized by RIG-I-MDA5 and TLR3 to induce IFN-I responses against viral infection (Goubau et al., 2013), and IFN-I response has been found to suppress RNAi by inhibiting RISC (Maillard et al., 2016; Seo et al., 2013). Moreover, many VSRS such as NoV B2 and IAV NS1 are dsRNA-binding proteins, and it remains unclear if the restricted replication and pathogenicity of mutant viruses are due to their inability to suppress viral siRNA production or IFN response. We also observed that 3A has a minor IFN-I suppression activity in cells. To exclude the potential interference of IFN-I, mammalian somatic cells or mice that are unable to mount IFN-I responses need to be challenged by WT and VSR-deficient viruses (Cullen et al., 2013). Indeed, VSR-deficient HEV71 triggered the production of readily detectable viral siRNAs in *Irfar1*^{-/-} MLFs and mice, and correspondingly, the replication and pathogenicity of the mutant virus were also dramatically restricted. In addition, when IFN-I response was blocked, the genetic ablation of Dicer still rescued the replication of VSR-deficient HEV71 both in vitro and ex vivo. Thus, 3A does protect HEV71 from antiviral RNAi independently of IFN response in mammals.

In conclusion, our findings demonstrate that HEV71 expresses protein 3A as VSR to effectively suppress the production of virally derived siRNAs and antiviral RNAi immunity in human somatic cell lines, murine primary somatic cells, and mice. To our best knowledge, our study is the first to demonstrate the production of readily detectable virus-derived siRNAs by WT Dicer in an IFN-independent manner in vivo, and our study further shows that these viral siRNAs have antiviral activity by loading into RISC and specifically silencing cognate viral RNA sequence. In addition, it uncovers for the first time the detailed mechanism by which a human positive-stranded RNA virus acts to evade antiviral RNAi both in vitro and in vivo. Based upon the data presented here and in previous studies, either enhancing the activity of the RNAi pathway or directly targeting VSRS like HEV71 3A may be promising strategies to develop novel antiviral therapies, and RNAi should function as an important antiviral immunity against more RNA viruses that include many important emerging and reemerging human pathogens, therefore representing an exciting avenue for future studies.

STAR★METHODS

Detailed methods are provided in the online version of this paper and include the following:

- **KEY RESOURCES TABLE**

- **CONTACT FOR REAGENT AND RESOURCE SHARING**
- **EXPERIMENTAL MODEL AND SUBJECT DETAILS**
 - Cell culture
 - Virus
 - Mice
- **METHOD DETAILS**
 - Plasmids and RNAs
 - Construction and recovery of HEV71 mutant viruses
 - Virus infection, plaque assays and IFA
 - RNA extraction, Northern blotting and qRT-PCR
 - Western blotting
 - CRISPR/Cas9 Knockout
 - Expression and purification of recombinant proteins, gel shift and in vitro Dicer cleavage assays
 - RNA-IP
 - Deep sequencing and data analysis
 - Mouse experiments
- **QUANTIFICATION AND STATISTICAL ANALYSIS**
- **DATA AND SOFTWARE AVAILABILITY**

SUPPLEMENTAL INFORMATION

Supplemental Information includes six figures and two tables and can be found with this article online at <http://dx.doi.org/10.1016/j.immuni.2017.05.006>.

AUTHOR CONTRIBUTIONS

Y.Q. and Y.X. performed experiments with the help of H.Z., Y.-Q.D., X.-F.L., F.-C.Z., and M.M.; Y.Z. analyzed the sequencing data; Q.Z. and B.Z. provided essential materials; Y.H. and L.W. helped with experimental design and data interpretation; Y.Q., C.-F.Q., and X.Z. designed the overall study, analyzed the data, and wrote the paper.

ACKNOWLEDGMENTS

We thank Bryan R. Cullen (Durham, NC), Hong-Bing Shu (Wuhan, China), Qi-Bin Leng (Shanghai, China), and Shou-wei Ding (Riverside, CA) for reagents. We also thank Ms. Markeda Wade (Houston, TX) for professionally editing the manuscript. This work was supported by the National Key Research and Development Project of China (2016YFD0500304 to C.-F.Q.), the NSFC Excellent Young Scientist Fund (No. 81522025 to C.-F.Q. and No. 31522004 to X.Z.), the National Basic Research Program of China (2014CB542603 to X.Z.), the NSFC No. 31670161 (to X.Z.), the Newton Advanced Fellowship from the UK Academy of Medical Sciences and NSFC (81661130162 to C.-F.Q. and 31761130075 to X.Z.), the Strategic Priority Research Program of Chinese Academy of Sciences (No. XDPB0301 to X.Z.), the National High-Tech R&D Program of China (2015AA020939 to X.Z.), the National Science and Technology Major Project of China (2017ZX09101005 and 2017ZX10304402), and the Open Research Fund of the State Key Laboratory of Pathogen and Biosafety of China (No. SKLPBS1445).

Received: January 17, 2017

Revised: April 9, 2017

Accepted: May 5, 2017

Published: June 20, 2017

REFERENCES

- Aliyari, R., Wu, Q., Li, H.W., Wang, X.H., Li, F., Green, L.D., Han, C.S., Li, W.X., and Ding, S.W. (2008). Mechanism of induction and suppression of antiviral immunity directed by virus-derived small RNAs in *Drosophila*. *Cell Host Microbe* 4, 387–397.
- Bogerd, H.P., Skalsky, R.L., Kennedy, E.M., Furuse, Y., Whisnant, A.W., Flores, O., Schultz, K.L., Putnam, N., Barrows, N.J., Sherry, B., et al.

- (2014a). Replication of many human viruses is refractory to inhibition by endogenous cellular microRNAs. *J. Virol.* **88**, 8065–8076.
- Bogerd, H.P., Whisnant, A.W., Kennedy, E.M., Flores, O., and Cullen, B.R. (2014b). Derivation and characterization of Dicer- and microRNA-deficient human cells. *RNA* **20**, 923–937.
- Carthew, R.W., and Sontheimer, E.J. (2009). Origins and Mechanisms of miRNAs and siRNAs. *Cell* **136**, 642–655.
- Cullen, B.R., Cherry, S., and tenOever, B.R. (2013). Is RNA interference a physiologically relevant innate antiviral immune response in mammals? *Cell Host Microbe* **14**, 374–378.
- Ding, S.W. (2010). RNA-based antiviral immunity. *Nat. Rev. Immunol.* **10**, 632–644.
- Flemer, M., Malik, R., Franke, V., Nejepinska, J., Sedlacek, R., Vlahovicek, K., and Svoboda, P. (2013). A retrotransposon-driven dicer isoform directs endogenous small interfering RNA production in mouse oocytes. *Cell* **155**, 807–816.
- Gao, Q., Yuan, S., Zhang, C., Wang, Y., Wang, Y., He, G., Zhang, S., Altmeyer, R., and Zou, G. (2015). Discovery of itraconazole with broad-spectrum in vitro antienterovirus activity that targets nonstructural protein 3A. *Antimicrob. Agents Chemother.* **59**, 2654–2665.
- García-Sastre, A., Egorov, A., Matassov, D., Brandt, S., Levy, D.E., Durbin, J.E., Palese, P., and Muster, T. (1998). Influenza A virus lacking the NS1 gene replicates in interferon-deficient systems. *Virology* **252**, 324–330.
- Goubau, D., Deddouche, S., and Reis e Sousa, C. (2013). Cytosolic sensing of viruses. *Immunity* **38**, 855–869.
- Haasnoot, J., de Vries, W., Geutjes, E.J., Prins, M., de Haan, P., and Berkhout, B. (2007). The Ebola virus VP35 protein is a suppressor of RNA silencing. *PLoS Pathog.* **3**, e86.
- Kennedy, E.M., Whisnant, A.W., Kornepati, A.V., Marshall, J.B., Bogerd, H.P., and Cullen, B.R. (2015). Production of functional small interfering RNAs by an amino-terminal deletion mutant of human Dicer. *Proc. Natl. Acad. Sci. USA* **112**, E6945–E6954.
- Kim, V.N., Han, J., and Siomi, M.C. (2009). Biogenesis of small RNAs in animals. *Nat. Rev. Mol. Cell Biol.* **10**, 126–139.
- Kim, S.W., Li, Z., Moore, P.S., Monaghan, A.P., Chang, Y., Nichols, M., and John, B. (2010). A sensitive non-radioactive northern blot method to detect small RNAs. *Nucleic Acids Res.* **38**, e98.
- Lei, C.Q., Zhong, B., Zhang, Y., Zhang, J., Wang, S., and Shu, H.B. (2010). Glycogen synthase kinase 3 β regulates IRF3 transcription factor-mediated antiviral response via activation of the kinase TBK1. *Immunity* **33**, 878–889.
- Li, H., Li, W.X., and Ding, S.W. (2002). Induction and suppression of RNA silencing by an animal virus. *Science* **296**, 1319–1321.
- Li, Y., Lu, J., Han, Y., Fan, X., and Ding, S.W. (2013). RNA interference functions as an antiviral immunity mechanism in mammals. *Science* **342**, 231–234.
- Li, Y., Basavappa, M., Lu, J., Dong, S., Cronkite, D.A., Prior, J.T., Reinecker, H.C., Hertzog, P., Han, Y., Li, W.X., et al. (2016). Induction and suppression of antiviral RNA interference by influenza A virus in mammalian cells. *Nat. Microbiol.* **2**, 16250.
- Li, C., Deng, Y.Q., Wang, S., Ma, F., Aliyari, R., Huang, X.Y., Zhang, N.N., Watanabe, M., Dong, H.L., Liu, P., et al. (2017). 25-Hydroxycholesterol Protects Host against Zika Virus Infection and Its Associated Microcephaly in a Mouse Model. *Immunity* **46**, 446–456.
- Liu, J., Carmell, M.A., Rivas, F.V., Marsden, C.G., Thomson, J.M., Song, J.J., Hammond, S.M., Joshua-Tor, L., and Hannon, G.J. (2004). Argonaute2 is the catalytic engine of mammalian RNAi. *Science* **305**, 1437–1441.
- Ma, E., MacRae, I.J., Kirsch, J.F., and Doudna, J.A. (2008). Autoinhibition of human dicer by its internal helicase domain. *J. Mol. Biol.* **380**, 237–243.
- Maillard, P.V., Ciaudo, C., Marchais, A., Li, Y., Jay, F., Ding, S.W., and Voinnet, O. (2013). Antiviral RNA interference in mammalian cells. *Science* **342**, 235–238.
- Maillard, P.V., Van der Veen, A.G., Deddouche-Grass, S., Rogers, N.C., Merits, A., and Reis e Sousa, C. (2016). Inactivation of the type I interferon pathway reveals long double-stranded RNA-mediated RNA interference in mammalian cells. *EMBO J.* **35**, 2505–2518.
- Mesa, R.A., Yasothan, U., and Kirkpatrick, P. (2012). Ruxolitinib. *Nat. Rev. Drug Discov.* **11**, 103–104.
- Nejepinska, J., Malik, R., Filkowski, J., Flemer, M., Filipowicz, W., and Svoboda, P. (2012). dsRNA expression in the mouse elicits RNAi in oocytes and low adenosine deamination in somatic cells. *Nucleic Acids Res.* **40**, 399–413.
- Parameswaran, P., Sklan, E., Wilkins, C., Burgon, T., Samuel, M.A., Lu, R., Ansel, K.M., Heissmeyer, V., Einav, S., Jackson, W., et al. (2010). Six RNA viruses and forty-one hosts: viral small RNAs and modulation of small RNA repertoires in vertebrate and invertebrate systems. *PLoS Pathog.* **6**, e1000764.
- Qi, N., Zhang, L., Qiu, Y., Wang, Z., Si, J., Liu, Y., Xiang, X., Xie, J., Qin, C.F., Zhou, X., and Hu, Y. (2012). Targeting of dicer-2 and RNAi by a viral RNA silencing suppressor in *Drosophila* cells. *J. Virol.* **86**, 5763–5773.
- Seo, G.J., Kincaid, R.P., Phanaksri, T., Burke, J.M., Pare, J.M., Cox, J.E., Hsiang, T.Y., Krug, R.M., and Sullivan, C.S. (2013). Reciprocal inhibition between intracellular antiviral signaling and the RNAi machinery in mammalian cells. *Cell Host Microbe* **14**, 435–445.
- Shih, S.R., Stollar, V., and Li, M.L. (2011). Host factors in enterovirus 71 replication. *J. Virol.* **85**, 9658–9666.
- Strauss, D.M., Glustrom, L.W., and Wuttke, D.S. (2003). Towards an understanding of the poliovirus replication complex: the solution structure of the soluble domain of the poliovirus 3A protein. *J. Mol. Biol.* **330**, 225–234.
- Tam, O.H., Aravin, A.A., Stein, P., Girard, A., Murchison, E.P., Cheloufi, S., Hodges, E., Anger, M., Sachidanandam, R., Schultz, R.M., and Hannon, G.J. (2008). Pseudogene-derived small interfering RNAs regulate gene expression in mouse oocytes. *Nature* **453**, 534–538.
- Teterina, N.L., Pinto, Y., Weaver, J.D., Jensen, K.S., and Ehrenfeld, E. (2011). Analysis of poliovirus protein 3A interactions with viral and cellular proteins in infected cells. *J. Virol.* **85**, 4284–4296.
- Watanabe, T., Totoki, Y., Toyoda, A., Kaneda, M., Kuramochi-Miyagawa, S., Obata, Y., Chiba, H., Kohara, Y., Kono, T., Nakano, T., et al. (2008). Endogenous siRNAs from naturally formed dsRNAs regulate transcripts in mouse oocytes. *Nature* **453**, 539–543.
- Weng, K.F., Hung, C.T., Hsieh, P.T., Li, M.L., Chen, G.W., Kung, Y.A., Huang, P.N., Kuo, R.L., Chen, L.L., Lin, J.Y., et al. (2014). A cytoplasmic RNA virus generates functional viral small RNAs and regulates viral IRES activity in mammalian cells. *Nucleic Acids Res.* **42**, 12789–12805.
- Wessels, E., Notebaart, R.A., Duijsings, D., Lanke, K., Vergeer, B., Melchers, W.J., and van Kuppeveld, F.J. (2006). Structure-function analysis of the coxsackievirus protein 3A: identification of residues important for dimerization, viral rna replication, and transport inhibition. *J. Biol. Chem.* **281**, 28232–28243.
- Zhang, M., Zhang, M.X., Zhang, Q., Zhu, G.F., Yuan, L., Zhang, D.E., Zhu, Q., Yao, J., Shu, H.B., and Zhong, B. (2016). USP18 recruits USP20 to promote innate antiviral response through deubiquitinating STING/MITA. *Cell Res.* **26**, 1302–1319.